Editors' Suggestion

Observation of an Excited Ω^- Baryon

J. Yelton,[10] I. Adachi,[19,15] J. K. Ahn,[39] H. Aihara,[85] S. Al Said,[79,37] D. M. Asner,[3] H. Atmacan,[75] T. Aushev,[54] R. Ayad,[79] V. Babu,[80] I. Badhrees,[79,36] S. Bahinipati,[23] A. M. Bakich,[78] V. Bansal,[66] C. Beleño,[14] M. Berger,[76] V. Bhardwaj,[22] B. Bhuyan,[24] T. Bilka,[5] J. Biswal,[34] A. Bondar,[4,64] G. Bonvicini,[89] A. Bozek,[61] M. Bračko,[48,34] T. E. Browder,[18] D. Červenkov,[5] V. Chekelian,[49] A. Chen,[58] B. G. Cheon,[17] K. Chilikin,[44] K. Cho,[38] S.-K. Choi,[16] Y. Choi,[77] S. Choudhury,[25] D. Cinabro,[89] S. Cunliffe,[8] T. Czank,[83] N. Dash,[23] S. Di Carlo,[42] Z. Doležal,[5] T. V. Dong,[19,15] Z. Drásal,[5] S. Eidelman,[4,64,44] D. Epifanov,[4,64] J. E. Fast,[66] B. G. Fulsom,[66] R. Garg,[67] V. Gaur,[88] N. Gabyshev,[4,64] A. Garmash,[4,64] M. Gelb,[35] A. Giri,[25] P. Goldenzweig,[35] D. Greenwald,[82] E. Guido,[32] J. Haba,[19,15] K. Hayasaka,[63] H. Hayashii,[57] S. Hirose,[55] W.-S. Hou,[60] K. Inami,[55] G. Inguglia,[8] A. Ishikawa,[83] R. Itoh,[19,15] M. Iwasaki,[65] Y. Iwasaki,[19] W. W. Jacobs,[27] H. B. Jeon,[41] S. Jia,[2] Y. Jin,[85] K. K. Joo,[6] T. Julius,[50] A. B. Kaliyar,[26] K. H. Kang,[41] G. Karyan,[8] Y. Kato,[55] C. Kiesling,[49] D. Y. Kim,[74] J. B. Kim,[39] K. T. Kim,[39] S. H. Kim,[17] K. Kinoshita,[7] P. Kodyš,[5] S. Korpar,[48,34] D. Kotchetkov,[18] P. Križan,[45,34] R. Kroeger,[51] P. Krokovny,[4,64] T. Kuhr,[46] R. Kumar,[70] A. Kuzmin,[4,64] Y.-J. Kwon,[91] J. S. Lange,[12] I. S. Lee,[17] S. C. Lee,[41] L. K. Li,[28] Y. B. Li,[68] L. Li Gioi,[49] J. Libby,[26] D. Liventsev,[88,19] M. Lubej,[34] T. Luo,[11] M. Masuda,[84] T. Matsuda,[52] D. Matvienko,[4,64,44] J. T. McNeil,[10] M. Merola,[31,56] K. Miyabayashi,[57] H. Miyata,[63] R. Mizuk,[44,53,54] G. B. Mohanty,[80] H. K. Moon,[39] T. Mori,[55] R. Mussa,[32] E. Nakano,[65] M. Nakao,[19,15] T. Nanut,[34] K. J. Nath,[24] Z. Natkaniec,[61] M. Niiyama,[40] N. K. Nisar,[69] S. Nishida,[19,15] H. Ono,[62,63] P. Pakhlov,[44,53] G. Pakhlova,[44,54] B. Pal,[3] S. Pardi,[31] H. Park,[41] S. Paul,[82] T. K. Pedlar,[47] R. Pestotnik,[34] L. E. Piilonen,[88] V. Popov,[44,54] M. Ritter,[46] G. Russo,[31] D. Sahoo,[80] Y. Sakai,[19,15] S. Sandilya,[7] L. Santelj,[19] T. Sanuki,[83] V. Savinov,[69] O. Schneider,[43] G. Schnell,[1,21] C. Schwanda,[29] Y. Seino,[63] K. Senyo,[90] M. E. Sevior,[50] V. Shebalin,[4,64] C. P. Shen,[2] T.-A. Shibata,[86] J.-G. Shiu,[60] B. Shwartz,[4,64] F. Simon,[49,81] A. Sokolov,[30] E. Solovieva,[44,54] M. Starič,[34] J. F. Strube,[66] M. Sumihama,[13] T. Sumiyoshi,[87] K. Suzuki,[76] M. Takizawa,[73,20,71] U. Tamponi,[32] K. Tanida,[33] Y. Tao,[10] F. Tenchini,[50] M. Uchida,[86] T. Uglov,[44,54] S. Uno,[19,15] P. Urquijo,[50] Y. Usov,[4,64] S. E. Vahsen,[18] C. Van Hulse,[1] G. Varner,[18] V. Vorobyev,[4,64,44] A. Vossen,[9] B. Wang,[7] C. H. Wang,[59] M.-Z. Wang,[60] P. Wang,[28] X. L. Wang,[11] M. Watanabe,[63] S. Watanuki,[83] E. Widmann,[76] E. Won,[39] H. Ye,[8] C. Z. Yuan,[28] Y. Yusa,[63] S. Zakharov,[44,54] Z. P. Zhang,[72] V. Zhilich,[4,64] V. Zhukova,[44,53] and V. Zhulanov[4,64]

(Belle Collaboration)

[1]*University of the Basque Country UPV/EHU, 48080 Bilbao*
[2]*Beihang University, Beijing 100191*
[3]*Brookhaven National Laboratory, Upton, New York 11973*
[4]*Budker Institute of Nuclear Physics SB RAS, Novosibirsk 630090*
[5]*Faculty of Mathematics and Physics, Charles University, 121 16 Prague*
[6]*Chonnam National University, Kwangju 660-701*
[7]*University of Cincinnati, Cincinnati, Ohio 45221*
[8]*Deutsches Elektronen–Synchrotron, 22607 Hamburg*
[9]*Duke University, Durham, North Carolina 27708*
[10]*University of Florida, Gainesville, Florida 32611*
[11]*Key Laboratory of Nuclear Physics and Ion-beam Application (MOE) and Institute of Modern Physics, Fudan University, Shanghai 200443*
[12]*Justus-Liebig-Universität Gießen, 35392 Gießen*
[13]*Gifu University, Gifu 501-1193*
[14]*II. Physikalisches Institut, Georg-August-Universität Göttingen, 37073 Göttingen*
[15]*SOKENDAI (The Graduate University for Advanced Studies), Hayama 240-0193*
[16]*Gyeongsang National University, Chinju 660-701*
[17]*Hanyang University, Seoul 133-791*
[18]*University of Hawaii, Honolulu, Hawaii 96822*
[19]*High Energy Accelerator Research Organization (KEK), Tsukuba 305-0801*
[20]*J-PARC Branch, KEK Theory Center, High Energy Accelerator Research Organization (KEK), Tsukuba 305-0801*
[21]*IKERBASQUE, Basque Foundation for Science, 48013 Bilbao*
[22]*Indian Institute of Science Education and Research Mohali, SAS Nagar, 140306*
[23]*Indian Institute of Technology Bhubaneswar, Satya Nagar 751007*
[24]*Indian Institute of Technology Guwahati, Assam 781039*
[25]*Indian Institute of Technology Hyderabad, Telangana 502285*

[26]Indian Institute of Technology Madras, Chennai 600036
[27]Indiana University, Bloomington, Indiana 47408
[28]Institute of High Energy Physics, Chinese Academy of Sciences, Beijing 100049
[29]Institute of High Energy Physics, Vienna 1050
[30]Institute for High Energy Physics, Protvino 142281
[31]INFN—Sezione di Napoli, 80126 Napoli
[32]INFN—Sezione di Torino, 10125 Torino
[33]Advanced Science Research Center, Japan Atomic Energy Agency, Naka 319-1195
[34]J. Stefan Institute, 1000 Ljubljana
[35]Institut für Experimentelle Kernphysik, Karlsruher Institut für Technologie, 76131 Karlsruhe
[36]King Abdulaziz City for Science and Technology, Riyadh 11442
[37]Department of Physics, Faculty of Science, King Abdulaziz University, Jeddah 21589
[38]Korea Institute of Science and Technology Information, Daejeon 305-806
[39]Korea University, Seoul 136-713
[40]Kyoto University, Kyoto 606-8502
[41]Kyungpook National University, Daegu 702-701
[42]LAL, Univ. Paris-Sud, CNRS/IN2P3, Université Paris-Saclay, Orsay
[43]École Polytechnique Fédérale de Lausanne (EPFL), Lausanne 1015
[44]P.N. Lebedev Physical Institute of the Russian Academy of Sciences, Moscow 119991
[45]Faculty of Mathematics and Physics, University of Ljubljana, 1000 Ljubljana
[46]Ludwig Maximilians University, 80539 Munich
[47]Luther College, Decorah, Iowa 52101
[48]University of Maribor, 2000 Maribor
[49]Max-Planck-Institut für Physik, 80805 München
[50]School of Physics, University of Melbourne, Victoria 3010
[51]University of Mississippi, University, Mississippi 38677
[52]University of Miyazaki, Miyazaki 889-2192
[53]Moscow Physical Engineering Institute, Moscow 115409
[54]Moscow Institute of Physics and Technology, Moscow Region 141700
[55]Graduate School of Science, Nagoya University, Nagoya 464-8602
[56]Università di Napoli Federico II, 80055 Napoli
[57]Nara Women's University, Nara 630-8506
[58]National Central University, Chung-li 32054
[59]National United University, Miao Li 36003
[60]Department of Physics, National Taiwan University, Taipei 10617
[61]H. Niewodniczanski Institute of Nuclear Physics, Krakow 31-342
[62]Nippon Dental University, Niigata 951-8580
[63]Niigata University, Niigata 950-2181
[64]Novosibirsk State University, Novosibirsk 630090
[65]Osaka City University, Osaka 558-8585
[66]Pacific Northwest National Laboratory, Richland, Washington 99352
[67]Panjab University, Chandigarh 160014
[68]Peking University, Beijing 100871
[69]University of Pittsburgh, Pittsburgh, Pennsylvania 15260
[70]Punjab Agricultural University, Ludhiana 141004
[71]Theoretical Research Division, Nishina Center, RIKEN, Saitama 351-0198
[72]University of Science and Technology of China, Hefei 230026
[73]Showa Pharmaceutical University, Tokyo 194-8543
[74]Soongsil University, Seoul 156-743
[75]University of South Carolina, Columbia, South Carolina 29208
[76]Stefan Meyer Institute for Subatomic Physics, Vienna 1090
[77]Sungkyunkwan University, Suwon 440-746
[78]School of Physics, University of Sydney, New South Wales 2006
[79]Department of Physics, Faculty of Science, University of Tabuk, Tabuk 71451
[80]Tata Institute of Fundamental Research, Mumbai 400005
[81]Excellence Cluster Universe, Technische Universität München, 85748 Garching
[82]Department of Physics, Technische Universität München, 85748 Garching
[83]Department of Physics, Tohoku University, Sendai 980-8578
[84]Earthquake Research Institute, University of Tokyo, Tokyo 113-0032
[85]Department of Physics, University of Tokyo, Tokyo 113-0033

[86]Tokyo Institute of Technology, Tokyo 152-8550
[87]Tokyo Metropolitan University, Tokyo 192-0397
[88]Virginia Polytechnic Institute and State University, Blacksburg, Virginia 24061
[89]Wayne State University, Detroit, Michigan 48202
[90]Yamagata University, Yamagata 990-8560
[91]Yonsei University, Seoul 120-749

(Received 23 May 2018; published 2 August 2018)

Using data recorded with the Belle detector, we observe a new excited hyperon, an Ω^{*-} candidate decaying into $\Xi^0 K^-$ and $\Xi^- K^0_S$ with a mass of $2012.4 \pm 0.7(\mathrm{stat}) \pm 0.6(\mathrm{syst})\ \mathrm{MeV}/c^2$ and a width of $\Gamma = 6.4^{+2.5}_{-2.0}(\mathrm{stat}) \pm 1.6(\mathrm{syst})$ MeV. The Ω^{*-} is seen primarily in $\Upsilon(1S)$, $\Upsilon(2S)$, and $\Upsilon(3S)$ decays.

DOI: 10.1103/PhysRevLett.121.052003

The Ω^- comprises three strange quarks. Its excited states have proved difficult to find. The Particle Data Group (PDG) [1] lists only one of them, the $\Omega(2250)$, in its summary tables, and it has a mass almost 600 MeV/c^2 higher than that of the ground state. In addition, the particle listings detail two other states for which the evidence of existence is considered to be "only fair," and they are at even higher masses. The gap in the spectrum is surprising, as there are negative-parity orbital excitations of many other baryons approximately 300 MeV/c^2 above their respective ground states, and the quark model [2–5], Skyrme model [6], and lattice gauge theory [7] all predict a $J^P = \frac{1}{2}^-$ and $J^P = \frac{3}{2}^-$ pair of excited Ω^- states with masses in the 2000 MeV/c^2 region.

A particular feature of Ω^- baryons are their zero isospin which means that $\Omega^{*-} \to \Omega^- \pi^0$ decays are highly suppressed, and this restricts the possible decays of excited states, with the largest expected decay mode for low-lying states being ΞK. Such decays are analogous to the $\Omega_c^0 \to \Xi_c^+ K^-$ decays recently discovered by the LHCb Collaboration [8] and confirmed soon after by the Belle Collaboration [9].

In this Letter, we present the results of a search for Ω^{*-} using a data sample of e^+e^- annihilations, corresponding to an integrated luminosity of 980 fb^{-1}, recorded by the Belle detector [10] operating at the KEKB asymmetric-energy e^+e^- collider [11]. The analysis concentrates on data taken with the accelerator energy tuned for the production of the $\Upsilon(1S)$, $\Upsilon(2S)$, and $\Upsilon(3S)$ resonances, with integrated luminosities of 5.7, 24.9, and 2.9 fb^{-1}, respectively. The decays of these narrow resonances proceed via gluons, and it has long been known that they contain an enhanced baryon fraction compared with continuum $e^+e^- \to q\bar{q}$ events [12–14].

We search for excited Ω^- decays into $\Xi^0 K^-$ and $\Xi^- \bar{K}^0$ [15], with subsequent decays into $\Xi^- \to \Lambda\pi^-$, $\Xi^0 \to \Lambda\pi^0$, $\bar{K}^0 \to \pi^+\pi^-$, $\Lambda \to p\pi^-$, and $\pi^0 \to \gamma\gamma$. An excited Ω^- would be expected to decay strongly, and, because of isospin symmetry, with almost equal branching fractions, into the above two decay modes, and they would likely dominate the decays of any Ω^{*-} with a mass between the ΞK and $\Xi(1530)K$ thresholds.

The Belle detector was a large solid-angle spectrometer comprising six subdetectors: the silicon vertex detector (SVD), the 50-layer central drift chamber (CDC), the aerogel Cherenkov counter (ACC), the time-of-flight scintillation counter (TOF), the electromagnetic calorimeter (ECL, divided into the barrel ECL in the central region and the forward and backward end caps at smaller angles with respect to the beam axis), and the K^0_L and muon detector. A superconducting solenoid produces a 1.5 T magnetic field throughout the first five of these subdetectors. The detector is described in more detail in Ref. [10]. Two inner detector configurations were used. The first comprised a 2.0 cm radius beam pipe and a 3-layer SVD and the second a 1.5 cm radius beam pipe and a 4-layer SVD and a small-cell inner CDC.

Charged particles $\pi^\pm$, K^-, and p are selected using the information from the tracking (SVD, CDC) and charged-hadron identification (CDC, ACC, TOF) systems combined into a likelihood $\mathcal{L}(h1\,{:}\,h2) = \mathcal{L}_{h1}/(\mathcal{L}_{h1} + \mathcal{L}_{h2})$, where h_1 and h_2 are p, K, and π as appropriate. Kaon candidates are defined as those with $\mathcal{L}(K\,{:}\,\pi) > 0.9$ and $\mathcal{L}(K\,{:}\,p) > 0.9$, which is approximately 83% efficient. For protons, the requirements are $\mathcal{L}(p\,{:}\,\pi) > 0.2$ and $\mathcal{L}(p\,{:}\,K) > 0.2$, while for charged pions $\mathcal{L}(\pi\,{:}\,p) > 0.2$ and $\mathcal{L}(\pi\,{:}\,K) > 0.2$; these requirements are approximately 99% efficient.

The π^0 candidates are reconstructed from two neutral clusters detected in the ECL, each consistent with being due to a photon and having an energy greater than 30 MeV in the laboratory frame (for those in the end cap calorimeter, the energy threshold is increased to 50 MeV).

Candidate $\Lambda(K^0_S)$ decays are made from $p\pi^-(\pi^+\pi^-)$ pairs with a production vertex significantly separated from the average interaction point (IP) and a reconstructed invariant mass within 3.5 (5.0) MeV/c^2 of the peak values.

Each Ξ^- candidate is reconstructed by combining a Λ candidates with a π^- candidate. The vertex formed from these two is required to be at least 0.35 cm from the IP, to be a shorter distance from the IP than the Λ decay vertex, and to signify a positive Ξ^- flight distance. The $\Xi^0 \to \Lambda\pi^0$ reconstruction is complicated by the fact that the π^0 has negligible vertex position information. Combinations of Λ and π^0 candidates are made, and then, assuming the IP to be production point of the Ξ^0, the sum of the Λ and π^0 momenta is taken as the momentum vector of the Ξ^0 candidate. The intersection of this trajectory with the reconstructed Λ trajectory is then found, and this position is taken as the decay location of the Ξ^0 hyperon. The π^0 is then remade from the two photons using this location as its point of origin. The reconstructed invariant mass of the π^0 candidate must be within 10.8 MeV/c^2 of the nominal mass (approximately 94% efficient). To reduce the large combinatorial background, the momentum of the π^0 candidate is required to be greater than 200 MeV/c. Combinations are retained if they have a decay location of the Ξ^0 indicating a positive Ξ^0 path length of greater than 2 cm but less than the distance between the Λ decay vertex and the IP. The refitting of the π^0 at the reconstructed Ξ^0 decay vertex improves the Ξ^0 mass resolution by around 15%.

The resultant invariant mass plots for the Ξ^0 and Ξ^- candidates are shown in Fig. 1. The red vertical arrows indicate the limits of the reconstructed invariant masses of the candidates retained for further analysis, which are ± 5.0 and ± 3.5 MeV/c^2 around the central values of the Ξ^0 and Ξ^- mass peaks, respectively, which are each approximately 95% efficient. For the Ξ^0, the value of the mass peak is 1.3155 GeV/c^2 and is higher than the PDG [1] value of $1.31\,486 \pm 0.00\,020$ GeV/c^2. This difference is later used in the estimate of the systematic uncertainty of the Ω^{*-} resonance mass measurement.

The Ξ^0 and Ξ^- candidates are kinematically constrained to their nominal masses [1] and then combined with K^- and K_S^0 candidates, respectively. The two particle combinations are kinematically constrained to come from a common vertex at the IP, and the χ^2 of this is required to be consistent with the daughters being produced by a common parent. For the $\Xi^0 K^-$ case, if there is more than one candidate with the same Λ and K^- but a different π^0, the one with the higher π^0 momentum is kept and others discarded to avoid double counting. This occurs around 3% of the time.

Figure 2 shows the $\Xi^0 K^-$ and $\Xi^- K_S^0$ invariant mass distributions in data taken at the $\Upsilon(1S)$, $\Upsilon(2S)$, and $\Upsilon(3S)$ resonance energies. Excesses are present in both distributions at around 2.01 GeV/c^2. It should be noted that real $\Xi^0 K^-$ combinations have three units of strangeness and are therefore highly suppressed. In contrast, $\Xi^- K_S^0$ combinations may have one unit of strangeness and thus have a larger combinatorial background.

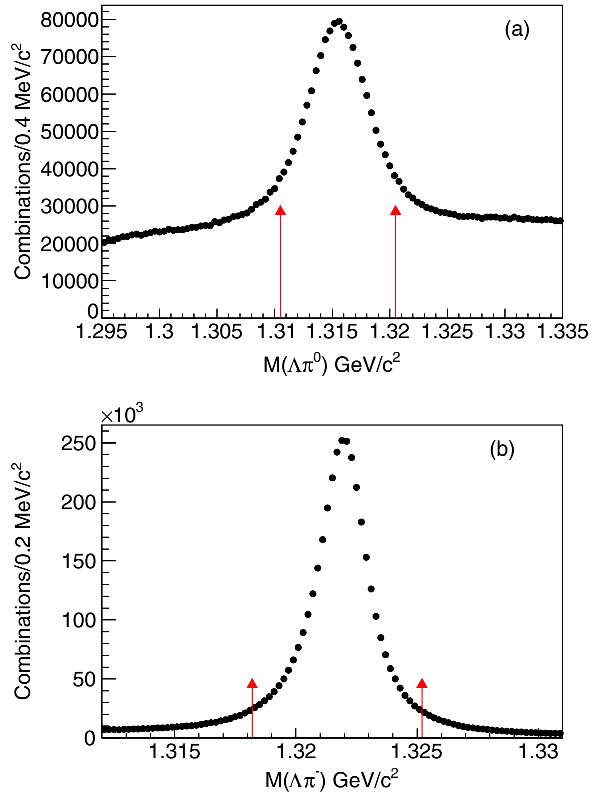

FIG. 1. Reconstructed invariant mass distributions, using all Belle data, of (a) $\Lambda\pi^0$ and (b) $\Lambda\pi^-$ combinations after all requirements. The arrows show the mass windows used for Ξ^0 and Ξ^- identification.

A simultaneous fit applied to the two distributions is shown in Fig. 2 and uses fitting functions where the signal functions are Voigtian functions (Breit-Wigners convolved with a Gaussian resolution functions) and the background functions second-order Chebyshev polynomials. The masses and intrinsic widths of the two Voigtian functions are kept the same. The resolution functions are obtained from Monte Carlo (MC) events, generated using EvtGen [16] with the Belle detector response simulated using the GEANT3 [17] framework, and parametrized as Gaussian distributions with widths of 2.27 MeV/c^2 for $\Xi^0 K^-$ and 1.77 MeV/c^2 for $\Xi^- K_S^0$. The fit is made to the binned invariant mass distributions with a large number of small bins, using the maximum-likelihood method. A convenient test of the goodness-of-fit is the χ^2 per degree of freedom (χ^2/d.o.f.) for the distribution plotted in 2.5 MeV/c^2 bins. The signal yields, mass, intrinsic width, and χ^2/d.o.f. resulting from this fit are listed in Table I. We calculate the statistical significance of the signal by excluding the peaks from the fit, finding the change in the log-likelihood ($\Delta[\ln(L)]$) and converting this to a p-value taking into account the change in d.o.f. This is then converted to an

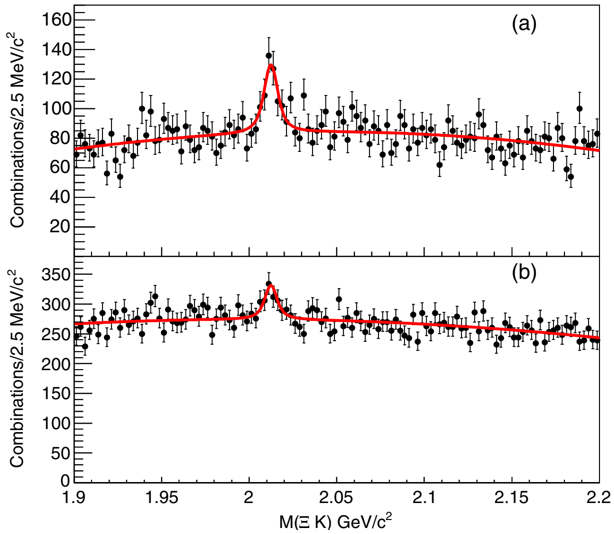

FIG. 2. The (a) $\Xi^0 K^-$ and (b) $\Xi^- K_S^0$ invariant mass distributions in data taken at the $\Upsilon(1S)$, $\Upsilon(2S)$, and $\Upsilon(3S)$ resonance energies. The curves show a simultaneous fit to the two distributions with a common mass and width.

effective number of standard deviations n_σ, and for this simultaneous fit, we find $n_\sigma = 8.3$.

Table I also lists results obtained from fitting to each of the two distributions separately. The signals in the $\Xi^0 K^-$ and $\Xi^- K_S^0$ mass distributions have significances of $n_\sigma = 6.9$ and $n_\sigma = 4.4$, respectively, and have statistically compatible masses and widths.

We have performed a series of checks to confirm the stability of the signal peak. Reasonable changes to the selection criteria of the daughter particles produce changes in the signal yield consistent with statistics. It would be surprising if an Ω^{*-} were not also produced in continuum $e^+e^- \to q\bar{q}$ events. In Fig. 3, we present mass distributions as in Fig. 2 but for the remainder of the Belle data, which comprise a total of 946 fb^{-1} taken mostly at the $\Upsilon(4S)$ energy but also in the continuum below and above this energy as well as at the $\Upsilon(5S)$. For the fits shown in Fig. 3, we use second-order Chebyshev background functions together with signal functions with mass and width fixed to the values found in the $\Upsilon(1S, 2S, 3S)$ data. Both distributions show excesses in the signal region, and their statistical significances are listed in Table I.

Taking into account the detection efficiency of the two modes, we use the results of the simultaneous fit to the $\Upsilon(1S, 2S, 3S)$ data to calculate the branching fraction ratio $\mathcal{R} = [\mathcal{B}(\Omega^{*-} \to \Xi^0 K^-)/\mathcal{B}(\Omega^{*-} \to \Xi^- \bar{K}^0)] = 1.2 \pm 0.3$, where statistical uncertainties dominate. With perfect isospin symmetry, this ratio would be 1, but the isospin mass splitting of the Ξ and K doublets will lead to an increase of up to approximately 15% depending on the spin associated with decay. The obtained value of $\mathcal{R}$ is consistent with the expectation.

The significance of the observation is largely unaffected by systematic uncertainties associated with the limited knowledge of the resolution and momentum scale of the detector. However, the use of different background functions can change the significance values. If we replace the background functions by third-order Chebyshev polynomials, the significance of the signal in the simultaneous fit is reduced to $n_\sigma = 7.2$. We take this value as the signal significance including systematic uncertainties. We also investigated the possibility of a further signal at around a mass of 1.95 GeV$/c^2$ where the data show an excess of events. This excess is not statistically significant ($n_\sigma < 3$), and its inclusion in the fit makes a negligible change to the significance of the signal at 2.012 GeV$/c^2$.

The dominant systematic uncertainty of the mass measurement is that due to the masses of the Ξ^0 and Ξ^- hyperons, which enter almost directly into the calculation of the Ω^{*-} mass. Conservatively, we take the difference between the reconstructed Ξ^0 mass and the PDG value 0.6 MeV$/c^2$. The Belle charged-particle momentum scale is very well understood, and the uncertainty in the Ω^{*-} mass measurement due to this is much smaller than 0.6 MeV$/c^2$. Similarly, changing the fit function to a relativistic Breit-Wigner has negligible effect on the mass value.

MC simulation is known to reproduce the resolution of mass peaks within 10% over a large number of different systems. The resultant systematic uncertainty in Γ from this source is ± 0.37 MeV. Changing the background shapes to third-order Chebyshev polynomials changes the measured value of Γ by 1.6 MeV, and this is the dominant contributor to the systematic uncertainty of the width.

The theoretical models [2–7] predict a $J^P = \frac{1}{2}^-$ and $J^P = \frac{3}{2}^-$ pair of excited Ω^- states in this mass region but with large differences in their mass predictions. Our value

TABLE I. The results of fits to the data shown in Fig. 2. The uncertainties shown are statistical only.

Data	Mode	Mass (MeV$/c^2$)	Yield	Γ(MeV)	χ^2/d.o.f.	n_σ
$\Upsilon(1S, 2S, 3S)$	$\Xi^0 K^-$, $\Xi^- K_S^0$ (simultaneous)	2012.4 ± 0.7	242 ± 48, 279 ± 71	$6.4^{+2.5}_{-2.0}$	227/230	8.3
$\Upsilon(1S, 2S, 3S)$	$\Xi^0 K^-$	2012.6 ± 0.8	239 ± 53	6.1 ± 2.6	115/114	6.9
$\Upsilon(1S, 2S, 3S)$	$\Xi^- K_S^0$	2012.0 ± 1.1	286 ± 87	6.8 ± 3.3	101/114	4.4
Other	$\Xi^0 K^-$	2012.4 (fixed)	209 ± 63	6.4 (fixed)	102/116	3.4
Other	$\Xi^- K_S^0$	2012.4 (fixed)	153 ± 89	6.4 (fixed)	133/116	1.7

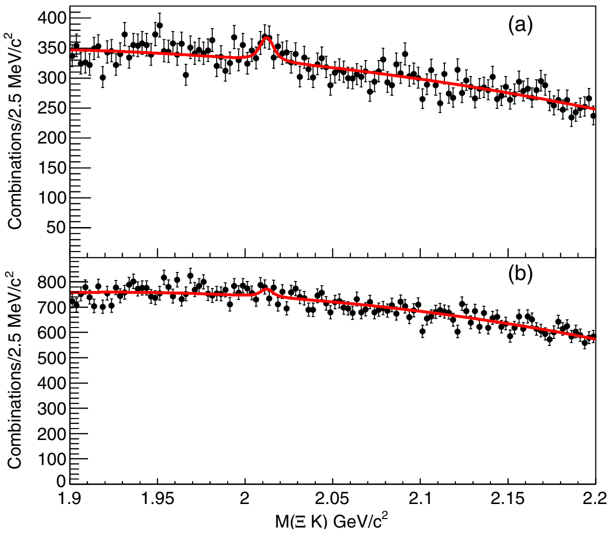

FIG. 3. The (a) $\Xi^0 K^-$, (b) $\Xi^- K_S^0$ invariant mass distributions in data taken at energies other than $\Upsilon(1S)$, $\Upsilon(2S)$, and $\Upsilon(3S)$ resonance energies. The curves show the result of independent fits to the two distributions with masses and widths fixed to those found by the fit shown in Fig. 2.

is, in general, closer to the those for the $J^P = \frac{3}{2}^-$ state. We also note that an Ω^{*-} with $J^P = \frac{3}{2}^-$ is restricted to decay to ΞK via a d wave, whereas a state with $J^P = \frac{1}{2}^-$ could decay via an s wave. Thus, the rather narrow width observed implies that the $\frac{3}{2}^-$ identification is more likely.

In summary, we have reported the observation of a new resonance, which we identify as an excited Ω^- baryon, found in the decay modes $\Omega^{*-} \to \Xi^0 K^-$ and $\Omega^{*-} \to \Xi^- K_S^0$. The measured mass of the resonance is $[2012.4 \pm 0.7\,(\mathrm{stat}) \pm 0.6\,(\mathrm{syst})]\ \mathrm{MeV}/c^2$, and its width Γ $[6.4^{+2.5}_{-2.0}\,(\mathrm{stat}) \pm 1.6\,(\mathrm{syst})\ \mathrm{MeV}]$. This new resonance has a mass $340\ \mathrm{MeV}/c^2$ higher than the ground state, and thus helps fill the large gap in the Ω^- spectrum between the ground state and the already observed excited states. It is found primarily in the decay of the narrow resonances $\Upsilon(1S)$, $\Upsilon(2S)$, and $\Upsilon(3S)$.

We thank the KEKB group for the excellent operation of the accelerator; the KEK cryogenics group for the efficient operation of the solenoid; and the KEK computer group, the National Institute of Informatics, and the Pacific Northwest National Laboratory (PNNL) Environmental Molecular Sciences Laboratory (EMSL) computing group for valuable computing and Science Information NETwork 5 (SINET5) network support. We acknowledge support from the Ministry of Education, Culture, Sports, Science, and Technology (MEXT) of Japan, the Japan Society for the Promotion of Science (JSPS), and the Tau-Lepton Physics Research Center of Nagoya University; the Australian Research Council; Austrian Science Fund under Grant No. P 26794-N20; the National Natural Science Foundation of China under Contracts No. 11435013, No. 11475187, No. 11521505, No. 11575017, No. 11675166, and No. 11705209; Key Research Program of Frontier Sciences, Chinese Academy of Sciences (CAS), Grant No. QYZDJ-SSW-SLH011; the CAS Center for Excellence in Particle Physics (CCEPP); Fudan University Grants No. JIH5913023, No. IDH5913011/003, No. JIH5913024, and No. IDH5913011/002; the Ministry of Education, Youth and Sports of the Czech Republic under Contract No. LTT17020; the Carl Zeiss Foundation, the Deutsche Forschungsgemeinschaft, the Excellence Cluster Universe, and the VolkswagenStiftung; the Department of Science and Technology of India; the Instituto Nazionale di Fisica Nucleare of Italy; National Research Foundation (NRF) of Korea Grants No. 2014R1A2A2A01005286, No. 2015R1A2A2A01003280, No. 2015H1A2A1033649, No. 2016R1D1A1B01010135, No. 2016K1A3A7A09005 603, and No. 2016R1D1A1B02012900; Radiation Science Research Institute, Foreign Large-size Research Facility Application Supporting project and the Global Science Experimental Data Hub Center of the Korea Institute of Science and Technology Information; the Polish Ministry of Science and Higher Education and the National Science Center; the Grant of the Russian Federation Government, Agreement No. 14.W03.31.0026, the Slovenian Research Agency; Ikerbasque, Basque Foundation for Science, Basque Government (Grant No. IT956-16) and Ministry of Economy and Competitiveness (MINECO) (Juan de la Cierva), Spain; the Swiss National Science Foundation; the Ministry of Education and the Ministry of Science and Technology of Taiwan; and the U. S. Department of Energy and the National Science Foundation.

[1] K. Olive *et al.* (Particle Data Group), Chin. Phys. C **40**, 100001 (2016), and 2017 update.
[2] S. Capstick and N. Isgur, Phys. Rev. D **34**, 2809 (1986).
[3] R. N. Faustov and V. O. Galkin, Phys. Rev. D **92**, 054005 (2015).
[4] U. Loring, B. Metsch, and H. Petry, Eur. Phys. J. A **10**, 447 (2001).
[5] M. Pervin and W. Roberts, Phys. Rev. C **77**, 025202 (2008).
[6] Y. Oh, Phys. Rev. D **75**, 074002 (2007).
[7] G. Engel, C. B. Lang, D. Mohler, and A. Schäfer (BGR Collaboration), Phys. Rev. D **87**, 074504 (2013).
[8] R. Aaij *et al.* (LHCb Collaboration), Phys. Rev. Lett. **118**, 182001 (2017).
[9] J. Yelton *et al.* (Belle Collaboration), Phys. Rev. D **97**, 051102 (2018).
[10] A. Abashian *et al.* (Belle Collaboration), Nucl. Instrum. Methods Phys. Res., Sect. A **479**, 117 (2002); see also detector section in J. Brodzicka *et al.*, Prog. Theor. Exp. Phys. **2012**, 4D001 (2012).
[11] S. Kurokawa and E. Kikutani, Nucl. Instrum. Methods Phys. Res., Sect. A **499**, 1 (2003), and other papers included in this volume; T. Abe *et al.*, Porg. Theor. Exp. Phys. **2013**, 03A001 (2013), and references therein.

[12] S. Behrends *et al.* (CLEO Collaboration), Phys. Rev. D **31**, 2161 (1985).

[13] H. Albrecht *et al.* (ARGUS Collaboration.), Z. Phys. C **39**, 177 (1989).

[14] R. Briere *et al.* (CLEO Collaboration), Phys. Rev. D **76**, 012005 (2007).

[15] Throughout this Letter, the inclusion of the charge-conjugate decay mode is implied unless otherwise stated.

[16] D. Lange, Nucl. Instrum. Methods Phys. Res., Sect. A **462**, 152 (2001).

[17] R. Brun *et al.* GEANT3.21, CERN Report DD/EE/84-1, 1984.